



## Impact of Heat Source/Sink towards MHD Stagnation Flow and Heat Transfer of GO-TiO<sub>2</sub>-Ag/Water Nanofluid over a Shrinking Surface

Nor Ain Azeany Mohd Nasir<sup>1,2,\*</sup>, Nooraini Zainuddin<sup>3</sup>, Norihan Md Arifin<sup>2,4</sup>, Nur Syahirah Wahid<sup>4</sup>, Ioan Pop<sup>5</sup>

<sup>1</sup> Department of Mathematics, Centre for Defence Foundation Studies, Universiti Pertahanan Nasional Malaysia, Kem Sungai Besi, 57000 Kuala Lumpur, Malaysia

<sup>2</sup> Institute for Mathematical Research, Universiti Putra Malaysia, 43400 Serdang, Selangor, Malaysia

<sup>3</sup> Department of Fundamental and Applied Sciences, Faculty of Science and Information Technology, Universiti Teknologi PETRONAS, 32610 Seri Iskandar, Perak, Malaysia

<sup>4</sup> Department of Mathematics and Statistics, Faculty of Science, Universiti Putra Malaysia, 43400 Serdang, Selangor, Malaysia

<sup>5</sup> Department of Mathematics, Babes-Bolyai University, 400084 Cluj-Napoca, Romania

### ARTICLE INFO

#### Article history:

Received 7 October 2024

Received in revised form 18 November 2024

Accepted 20 December 2024

Available online 31 January 2025

#### Keywords:

Ternary hybrid nanofluid; shrinking surface; heat source/sink; MHD

### ABSTRACT

This investigation aims to solve the mathematical modelling of magnetohydrodynamic (MHD) stagnation flow and heat transfer of GO-TiO<sub>2</sub>-Ag/water nanofluid towards a shrinking surface problem. The model contains the impacts of suction/injection, radiation, magnetic field intensity and heat source/sink parameters. By converting the governing equations into ordinary differential equations with applying similarity conversion and employing the *bvp4c* built-in solver in MATLAB software, numerical results are attained. Furthermore, the existence of GO as the ternary particles improves more the temperature profile but declining the velocity profile. This investigation promotes substantial understandings into heat transference achievement in MHD stagnation flow towards a shrinking surface, specifically with the interaction of GO particles and heat source/sink influences.

## 1. Introduction

Magnetohydrodynamic (MHD) stagnation flow is an essential domain of research in fluid dynamics, specifically when studying heat transfer anomaly. This flow system happens at the point where a fluid obtrudes on a solid plane, initiating a stagnation point. Nevertheless, when a magnetic field is directed to it, it causes electrical conductivity in the fluid, indicating complex connections between the fluid, magnetic field and solid surface at the stagnation point. Recognizing MHD stagnation flow is vital because of its significance in countless engineering utilizations, such as in aerospace engineering and material processing. For aerospace engineering, the MHD influences on stagnation flow are critical for planning re-entry vehicles and administering heat transferal through atmospheric entry. Managing heat transferal at stagnation points can change product quality and effectiveness in materials processing, such as crystal development or metal modelling. Due to its

\* Corresponding author.

E-mail address: [norainazeany@upnm.edu.my](mailto:norainazeany@upnm.edu.my) (Nor Ain Azeany Mohd Nasir)

<https://doi.org/10.37934/cfdl.17.7.142156>

significance in abundant domains, countless researchers have administered investigation on MHD. For precedent, Idris *et al.*, [1] discovered that enhancing the MHD parameter driven to a heat transferal ratio improvement of above 9%, whereas Rafique *et al.*, [2] declared an identical result, nevertheless, they also observed a reduce in the viscosity of the hybrid nanofluid. It is also important to concentrate on the details administered by Mumtaz *et al.*, [3], which declares that skin friction is enhanced concurrently with the MHD impact and the influence is superior when utilizing a ternary hybrid nanofluid. Mahmood *et al.*, [4] added to the literature that with the bits of help of MHD, the skin friction and heat transfer rate amplified together the volume fraction nanoparticles for the case using  $\text{Al}_2\text{O}_3\text{-Cu-TiO}_2/\text{H}_2\text{O}$  only. Furthermore, the flow of the fluid can be improved by adding more effects to the system, such as slip and suction factors, as demonstrated by Hussain *et al.*, [5]. Several other factors have been proposed to improve further the heat transfer rate, for instance, thermal stratification with mixed convection by Jamrus *et al.*, [6], hall current overheated rotating geometry by Ayub *et al.*, [7] and heat generation, viscous dissipation and joule heating effects by Rafique *et al.*, [8].

The importance of radiation effects in optimising ternary hybrid nanofluid flow and heat transfer lies in several key aspects. The radiation portrays a considerable part in the heat transferal procedure, exceptionally in circumstances where regular conduction and convection processes may be constrained. The presence of radiation influences can indicate enhanced thermal efficiency and heat transferal rates in nanofluid-based systems. This statement was confirmed when Wahid *et al.*, [9] stated that their research findings emphasized the efficiency of enhancing the boundary suction parameter and reduction thermal radiation leads to improve heat transferal within the certain conditions of a ternary hybrid nanofluid. In real-life relevance, the implication of radiation influences in fluid flow and heat transferal is apparent across diverse areas. For instance, in solar thermal systems where nanofluids are exploited as heat transferal fluids, radiation influences can drastically influence system effectiveness and energy gain. This anomaly can indicate further effective solar collectors and thermal energy storing systems. Furthermore, in manufacturing such as aerospace and automotive engineering, where thermal administration is essential for attainment and reliability, radiation outcomes play a critical part. It is stated that radiation can advance to superior cooling attainment, lessen energy utilization and improve system endurance in high-temperature environments. As Maranna *et al.*, [10] indicated, using second-grade fluid as the ternary hybrid nanofluid will ideally enhance the thermal layer with high-temperature profiles. A similar finding has been reported by Mahabaleshwar *et al.*, [11], with added to the report results revealing that the heat transfer performance of the ternary nanofluid phase is better than that of the dusty phase. Furthermore, in medical applications such as hyperthermia treatment, where precise control of temperature distribution is critical, radiation effects can be utilised to optimise heat transfer within nanofluid-based systems, leading to more effective therapeutic outcomes. Sharma *et al.*, [12] proposed that their discovery provides advantages for clinical researchers, as their study observed an increase in entropy generation and the Bejan number with the enhancement of the Brinkman and radiation parameters. Numerous researchers have investigated the impact of radiation towards ternary hybrid nanofluid flows in various circumstances, resulting in diverse findings. For instance, Aich *et al.*, [13] investigated the heat capacity for  $\text{Al}_2\text{O}_3\text{-CuO-Cu/water}$ , while Ali *et al.*, [14] considered the ternary hybrid Casson fluid over a nonlinear stretching disk.

Understanding and improving the effect of heat absorption/generation can result in improved heat management and enhanced performance in various engineering applications. Mahmood *et al.*, [15] proposed that investigating heat absorption/ generation can provide scientists and engineers with a starting point for optimising the relevant parameters to achieve optimal outcomes in practical applications. In real-life practices, the importance of heat generation/absorption outcomes in fluid

flow and heat transfer is obvious within varied industries. For illustration, in the area of energy generation, enhancing heat generation/absorption outcomes can increase the effectiveness of thermal power plants and improve energy conversion procedures. It is significant to recognize which influences can increase the heat transfer rate. For instance, Sajid *et al.*, [16] recommended that heat generation and absorption with the facilitate of the radiation outcome can enhance the heat transfer rate. Furthermore, in industries such as materials processing and manufacturing, where specific controller of temperature and heat transfer is improved for product worth and efficacy, augmenting heat generation/absorption impacts can lead to improvements in product progress, process optimisation and overall output. Numerous parameters have been attained that can dominate heat transfer jointly with heat absorption/generation, such as Casson fluid, thermal conductivity of the fluid, diffusion coefficient and wedge parameter, as disclosed by Sajid *et al.*, [17]. Additionally, in medical areas such as biomedical engineering, manipulating heat generation/absorption impacts are critical for medical device design. In authorization with this appliance, Alqahtani *et al.*, [18] have explored energy transport using Carreau Yasuda fluid. The findings affirmed that the magnetic dipole portrays a substantial role with the heat absorption/generation in improving the thermal energy transference of trihybrid nanofluid and dropping the velocity profile. Then, the investigation was further improved with the Fourier heat flux model over a disk by Alqawasmi *et al.*, [19], who observed that reducing the magnetic parameter decreases fluid velocity but increases fluid temperature over a spinning disc, with notable effects on temperature distribution and heat absorption/generation, particularly significant for ternary composite nanofluid. The latest finding by Mishra *et al.*, [20], demonstrated that the heat transfer rate is the highest for the cone surface rather than the flat surface when heat absorption/generation acts on the surface.

Based on the above-mentioned literature, this study intends to assess the ternary hybrid nanofluid flow and heat transfer of magnetohydrodynamic (MHD) at the stagnation point on a shrinking sheet. The impacts acting on the system involved in this study are assumed to be radiation and heat absorption/generation factors. The governing equations derived based on the problem mentioned above are then reduced to higher-order ordinary differential equations (ODEs) coupled with a boundary value problem. The ODEs are then solved using the famous solver called *bvp4c*, which is built into MATLAB software. The stability of the solutions has been shown by Wahid *et al.*, [21]. Hence, the results for the second solution will not be discussed but will still be reported since the flow might be useful in future and to avoid the misconstruction of the flow and heat transfer characteristics [22].

## 2. Methodology

A steady two-dimensional MHD stagnation-point flow of a ternary hybrid nanofluid towards the shrinkage surface is shown in Figure 1. In the Cartesian coordinate system, the  $x$  and  $y$  axes represent dimensions where the  $x$ -axis runs parallel to the surface and the  $y$ -axis extends in a direction that is perpendicular to the surface. The initiation of the flow occurs at  $y \geq 0$ . It is assumed that the velocity of the inviscid flow is  $u_e(x)$ , while the velocity of the retracting sheet is  $u_w(x)$ . It is also notable that  $v = v_0$  is the mass flux where  $v_0$  is known as injection parameter (positive), suction parameter (negative) and permeable (equals to zero). Considering the surface-normal direction of the transverse magnetic field is denoted by  $B_0$ , the temperature of the free stream is represented by  $T_\infty$  and the temperature of the sheet is denoted as  $T_w$ . It is also noted that viscous dissipation occurs when the internal friction within a fluid, caused by the relative motion of adjacent layers, results in the generation of heat. This energy dissipation process is taken into account in the energy equation.

Since the medium is impenetrable to radiation, Rosseland's approximation,  $q_r = -\frac{16\sigma^*T_\infty^3}{3k^*}\left(\frac{\partial T}{\partial y}\right)$  is used to model the radiative heat transfer where  $\sigma^*$  and  $k^*$  are Stefan-Boltzmann constant and mean absorption. Internal heat source or sink  $Q$ , which can affect the overall heat balance, is also considered. It is known that when  $Q > 0$  is assumed as heat source and  $Q < 0$  is assumed as heat sink.

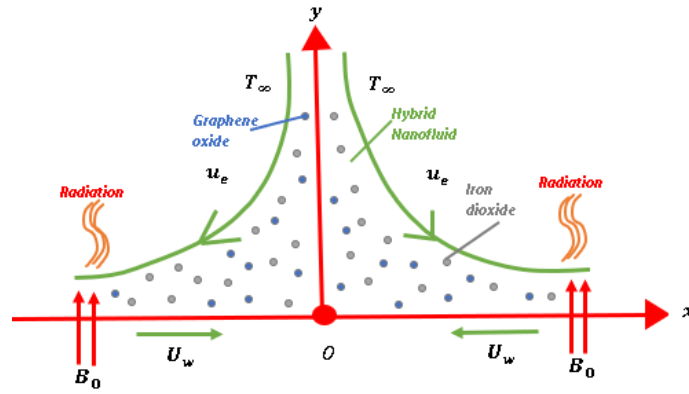


Fig. 1. Physical model for shrinking surface

The governing equations that dictate the assumptions regarding flow, as previously mentioned, can be outlined as follows, according to Wahid *et al.*, [21].

$$\frac{\partial u}{\partial x} + \frac{\partial v}{\partial y} = 0, \quad (1)$$

$$u \frac{\partial u}{\partial x} + v \frac{\partial u}{\partial y} = u_e \frac{du_e}{dx} + \frac{\mu_{thnf}}{\rho_{thnf}} \left( \frac{\partial^2 u}{\partial y^2} \right) - \frac{\sigma_{thnf} B_0^2}{\rho_{thnf}} (u - u_e), \quad (2)$$

$$u \frac{\partial T}{\partial x} + v \frac{\partial T}{\partial y} = \frac{k_{hnf}}{(\rho C_p)_{hnf}} \left( \frac{\partial^2 T}{\partial y^2} \right) + \frac{\mu_{hnf}}{(\rho C_p)_{hnf}} \left( \frac{\partial u}{\partial y} \right)^2 - \frac{1}{(\rho C_p)_{hnf}} \frac{\partial q_r}{\partial y} + \frac{Q}{(\rho C_p)_{thnf}} (T - T_\infty), \quad (3)$$

An adequate boundary condition, when combined,

$$\begin{aligned} u = u_w(x) = bx, \quad v = v_0, \quad T = T_w \quad \text{at } y = 0, \\ u \rightarrow u_e(x) = ax, \quad T \rightarrow T_\infty \quad \text{as } y \rightarrow \infty. \end{aligned} \quad (4)$$

The text outlines that the symbols  $\mu, \rho, \sigma, \rho C_p, k$  represent dynamic viscosity, density, electrical conductivity, heat capacity and thermal conductivity, correspondingly. The notation *thnf* is used to denote ternary hybrid nanofluid, with  $\phi_1, \phi_2$  and  $\phi_3$  indicating the volume percentages of graphene oxide (GO), titanium dioxide (TiO<sub>2</sub>) and silver (Ag) nanoparticles, respectively. Water (H<sub>2</sub>O) is utilised as the base fluid. Table 1 presents a detailed examination of the relationship between the thermophysical properties and the composition of ternary hybrid nanofluids.

**Table 1**

The correlation between the thermophysical properties of ternary hybrid nanofluids and the shape factors of their nanoparticles

Properties	Ternary Hybrid nanofluid
Density	$\frac{\rho_{thnf}}{\rho_f} = (1 - \phi_3) \left[ (1 - \phi_2) \left\{ (1 - \phi_1) + \phi_1 \frac{\rho_{s1}}{\rho_f} \right\} + \phi_2 \frac{\rho_{s2}}{\rho_f} \right] + \phi_3 \frac{\rho_{s3}}{\rho_f}$
Dynamic viscosity	$\frac{\mu_{thnf}}{\mu_f} = \frac{1}{(1 - \phi_1)^{2.5} (1 - \phi_2)^{2.5} (1 - \phi_3)^{2.5}}$
Electrical Conductivity	$\frac{\sigma_{thnf}}{\sigma_f} = \left[ \frac{(1 + 2\phi_2)\sigma_{s3} + (1 - 2\phi_3)\sigma_{hnf}}{(1 - \phi_2)\sigma_{s3} + (1 - \phi_3)\sigma_{hnf}} \right] \frac{\sigma_{hnf}}{\sigma_f}$ where $\frac{\sigma_{hnf}}{\sigma_{nf}} = \frac{\sigma_{s2} + 2\sigma_{nf} - 2\phi_2(\sigma_{nf} - \sigma_{s2})}{\sigma_{s2} + 2\sigma_{nf} + \phi_2(\sigma_{nf} - \sigma_{s2})}$ and $\frac{\sigma_{nf}}{\sigma_f} = \frac{\sigma_{s1} + 2\sigma_f - 2\phi_1(\sigma_f - \sigma_{s1})}{\sigma_{s1} + 2\sigma_f + \phi_1(\sigma_f - \sigma_{s1})}$
Heat capacity	$\frac{(\rho C_p)_{thnf}}{(\rho C_p)_f} = (1 - \phi_3) \left[ (1 - \phi_2) \left\{ (1 - \phi_1) + \phi_1 \frac{(\rho C_p)_{s1}}{(\rho C_p)_f} \right\} + \phi_2 \frac{(\rho C_p)_{s2}}{(\rho C_p)_f} \right] + \phi_3 \frac{(\rho C_p)_{s3}}{(\rho C_p)_f}$
Thermal conductivity	$\frac{k_{thnf}}{k_f} = \left[ \frac{k_{s3} + 2k_{hnf} - 2(k_{hnf} - k_{s3})\phi_3}{k_{s3} + 2k_{hnf} + (k_{hnf} - k_{s3})\phi_3} \right] \left( \frac{k_{hnf}}{k_f} \right)$ where $\frac{k_{hnf}}{k_{nf}} = \frac{k_{s2} + (m-1)k_{nf} - (m-1)(k_{nf} - k_{s2})\phi_2}{k_{s2} + (m-1)k_{nf} + (k_{nf} - k_{s2})\phi_2}$ and $\frac{k_{nf}}{k_f} = \frac{k_{s1} + (m-1)k_f - (m-1)(k_f - k_{s1})\phi_1}{k_{s1} + (m-1)k_f + (k_f - k_{s1})\phi_1}$

(Ref. Mumtaz *et al.*, [3])

Table 2 presents the data for computing the thermophysical characteristics of the hybrid nanofluid, as listed in Table 1.

**Table 2**

Thermophysical properties values of GO, TiO<sub>2</sub>, Ag and H<sub>2</sub>O

Thermophysical Properties	GO	TiO <sub>2</sub>	Ag	H <sub>2</sub> O
Dynamic viscosity $\mu$ ( $kgm^{-1}s^{-1}$ )	-	-	-	0.000855
Density $\rho$ ( $kgm^{-2}$ )	1800	4250	10500	997.1
Electrical Conductivity $\sigma$ ( $Sm^{-1}$ )	$6.3 \times 10^7$	$2.6 \times 10^6$	$6.3 \times 10^7$	$5.5 \times 10^{-6}$
Specific Heat capacity $C_p$ ( $Jkg^{-1}K^{-1}$ )	717	686	235	4179
Thermal conductivity $k$ ( $Wm^{-1}K^{-1}$ )	5000	8.9538	429	0.613

(Ref. Redouane *et al.*, [23])

To simplify the complexity of solving the mathematical modelling Eq. (1) to Eq. (4), they must be condensed into ordinary differential equations (ODEs). This can be efficiently done through the employment of similarity transformation, which involves the use of a suitable similarity variable, as detailed by Wahid *et al.*, [21].

$$\psi = \sqrt{av_f}xf(\eta), \quad \theta(\eta) = \frac{T - T_w}{T_w - T_\infty}, \quad \eta = \sqrt{\frac{a}{v_f}}y. \tag{5}$$

The stream function is associated with velocity components as given,

$$u = axf'(\eta), \quad v = -\sqrt{av_f}f(\eta). \tag{6}$$

By differentiating and substituting Eq. (5) and Eq. (6) into Eq. (1) through Eq. (4), new equations can be derived.

$$\frac{\phi_3}{\phi_4}f'''' - f'^2 + ff'' - \frac{\phi_5}{\phi_4}M(f' - 1) + 1 = 0, \tag{7}$$

$$\frac{1}{\phi_2 Pr} [\phi_1 + Rd] \vartheta'' + \frac{\phi_3}{\phi_2} Ec f''^2 + \frac{\xi}{\phi_2} \vartheta + f \vartheta' = 0, \quad (8)$$

along with an appropriate boundary condition,

$$\begin{aligned} f' = \alpha, \quad f = S, \quad \vartheta = 1 \quad \text{at } \eta = 0, \\ f' \rightarrow 1, \quad \vartheta \rightarrow 0 \quad \text{as } \eta \rightarrow \infty. \end{aligned} \quad (9)$$

In Eq. (7) to Eq. (9), the parameter is defined as per Table 3.

**Table 3**

List of parameters associated with Eq. (7) to Eq. (9)

Parameter	Equation
Magnetic parameter, $M$	$M = \frac{\sigma_f B_0^2}{a \rho_f}$
Ternary hybrid nanofluid parameter	$\phi_1 = \frac{k_{thnf}}{k_f}, \phi_2 = \frac{(\rho C_p)_{thnf}}{(\rho C_p)_f}, \phi_3 = \frac{\mu_{thnf}}{\mu_f}, \phi_4 = \frac{\rho_f}{\rho_{thnf}}, \phi_5 = \frac{\sigma_{thnf}}{\sigma_f}$
Radiation parameter, $Rd$	$Rd = \frac{16\sigma^* T_\infty^3}{3k^* k_f}$
Eckert number, $Ec$	$Ec = \frac{au_w^2}{(T_w - T_\infty)(C_p)_f}$
Heat source/sink, $\xi$	$\xi = \frac{Qa}{(\rho C_p)_f}$
Suction/injection parameter, $S$	$S = \frac{v_0}{-\sqrt{av_f}}$
Stretching/shrinking parameter, $\alpha$	$\alpha = \frac{b}{a}$

The physical quantities essential to Eq. (7) to Eq. (9) are recognised as skin friction and the Nusselt number.

$$\text{Skin friction } C_f = \frac{\mu_{thnf}}{\rho_f u_e^2} \left( \frac{\partial u}{\partial y} \right)_{y=0}, \quad (10)$$

$$\text{local Nusselt number } Nu_x = - \frac{x k_{thnf}}{k_f (T_w - T_\infty)} \left( \frac{\partial T}{\partial y} \right)_{y=0}.$$

Arranging the Eq. (10) and substituting Eq. (5) give out,

$$Re_x^{1/2} C_f = \phi_3 f''(0) \text{ and } Re_x^{-1/2} Nu_x = -\phi_1 \theta'(0), \quad (11)$$

where  $Re_x = u/v_f$  is Reynold's number.

### 3. Results

Using the `bvp4c` solver within MATLAB software, the system of equations, including the Eq. (7) and Eq. (8), along with the specified boundary conditions Eq. (9), is solved numerically. The `bvp4c` solver is embedded with the collocation method named 3 stage Lobatto method which known as a Runge Kutta family. It is generally acknowledged that the Runge Kutta family possessed a high accuracy and consistency computed solution. In order to maintain the convergence of the method,

the convergence criteria are set to  $TOL = 10^{-10}$ . Based on the numerical results,  $\eta = 10$  is sufficient to ensure the solutions are converged. The numerical results are presented through tables and figures. Precisely, Table 4 displays the relative values of the reduced skin friction coefficient for several values of parameters when  $\phi_3 = \phi_4 = 1, M = S = 0$ . These results indicate a significant agreement between the current findings and previous studies conducted by Aminuddin *et al.*, [24] and Nasir *et al.*, [25]. The established numerical approach demonstrates confidence in solving the current problem. Notably, the nanoparticle concentration and heat source/sink parameters considered in this study are within the ranges  $0 \leq \phi_3 \leq 0.03$  and  $-0.03 \leq \xi \leq 0.03$ , with the magnetic parameter  $0.01 \leq M \leq 0.07$ , the radiation parameter  $0.0 \leq Rd \leq 1.5$  and an Eckert number of  $0.1 \leq Ec \leq 0.3$ .

**Table 4**

Numerical solution for skin friction when  $\varphi_1 = \varphi_2 = \varphi_3 = 0, M = \xi = S = 0, Rd = 0, Ec = 0, \alpha = 0$  and  $Pr = 6.2$  (water)

$\alpha$	Aminuddin <i>et al.</i> , [24]		Nasir <i>et al.</i> , [25]		Current solution	
	Upper solution	Lower solution	Upper solution	Lower solution	Upper solution	Lower solution
-0.25	402240775	-	1.40224078	-	1.402240807	-
-0.5	1.495669733	-			1.495669765	-
-0.75	1.489298201	-	1.48929820	-	1.489298236	-
-1.0	1.328816835	0.000000000	1.32881685	0.0	1.328816875	0.0
-1.1	1.186680243	0.049228914	1.1866805	0.049229	1.186680258	0.049228955
-1.15	1.082231127	1.8223113	0.11670214	0.1167022	1.082231136	0.116701735
-1.2	0.932473313	0.233649705	0.93247331	0.23364973	0.932473318	0.233647245
-1.2465	0.584281488	0.554296326	0.58428116	0.55429619	0.584281486	0.553572833
-1.24657					0.574525287	0.562136224

### 3.1 Skin Friction Coefficient and Nusselt Number

Based on the numerical results illustrated in Table 5, it is evident that the magnetic parameter  $M$  have significantly affected skin friction. It is due to the Lorentz force induced by  $M$  which can significantly alter the flow patterns with the bits of help of the particles of ternary hybrid nanofluid. The impact is further amplified when the system has heat source parameters. For this problem, the heat source uniforms the heating process, smoothing the flow and resulting in reduced skin friction. This finding is aligned with results reported by Akaje *et al.*, [26]. It is noted that the suction parameter tends to pull the fluid towards the surface by altering the boundary layer thickness and the fluid flow velocity. This phenomenon leads to the augmentation of the Nusselt number. The radiation parameter further influences the heat transport ratio of the fluid flow. The radiation parameter contributes to the changes in temperature profile and heat dissipation, while the Eckert number would lead to variations in flow patterns and temperature differences, which would further affect the heat transportation ratio, hence reducing the skin friction on the shrinking surface.

However, it is well known that radiation can influence thermal energy transportation in fluid flow. It is eye-catching that the radiation parameter can further reduce the heat transportation ratio, as shown in Table 5. When the surface is shrinking, a higher radiation parameter leads to a decline in the Nusselt number. The reason for this is that higher radiation levels with the combination of magnetic, Eckert number and suction parameters result in more heat dispersion from the surface, decreasing the total heat transport rate to the fluid. As the Eckert number ascends, it indicates a greater dominance of thermal energy over kinetic energy in the fluid. This finding is contradicted with Kumar *et al.*, [27] due to the fact that they consider the case for stretching surface. It is acknowledged

that the effects will be different when difference case such as stretching and shrinking surface are involved. An augmentation in the Eckert number coupled with an elevated magnetic parameter might result in diminished Nusselt numbers on a shrinking surface. The reason for this is that the combined influence of magnetic forces and increased thermal energy can facilitate the dispersion of heat away from the surface, resulting in a decrease in the Nusselt number.

**Table 5**

Numerical results for skin friction coefficient and Nusselt number for various values of several parameters when  $\alpha = -2.5, S = 2.0, \varphi_1 = 0.01, \varphi_2 = \varphi_3 = 0.02, \xi = 0.1$ (heat source) and  $Pr = 6.2$  where [ ] indicate lower solution

$M$	$Rd$	$Ec$	$C_f$	$Nu_x$
0.01	0.5	0.1	6.593368585, [0.843041148]	0.428775204, [-20.974511337]
0.04			6.507550744, [0.908656715]	0.465482092, [-15.561502660]
0.07			6.419172005, [0.977360124]	0.502646827, [-11.884957299]
0.04	0.0		6.507550739, [0.908656712]	0.852023272, [-44.506121539]
	0.5		6.507550744, [0.908656715]	0.465482092, [-15.561502660]
	1.0		6.507550744, [0.908656724]	0.303238002, [-7.064164377]
	1.5		6.507550740, [0.908656729]	0.227372169, [-3.880797949]
	1.0	0.1	6.507550744, [0.908656724]	0.303238002, [-7.064164377]
		0.2	6.507550754, [0.908656715]	-4.665105047, [-16.619604371]
		0.3	6.507550756, [0.908656714]	-9.633448097, [-26.175044376]

Corresponding to the computed data exposed in Table 6, the occurrence of a magnetic field can affect in a decline in skin friction when heat sunk. The Lorentz force can resist the frictional forces exist in the fluid, indicating to a further streamlined flow over the contracting surface. In additive, the enclosure of a heat sink can also affect skin friction, thus improving the complexity of the condition. Joining heat sunk with suction create further reduction skin friction by enhancing the stability of flow and diminishing disorders in the flow. It is notable that heat sunk triggers a decline in thermal energy in the fluid, indicating to a decline in Nusselt number. Likewise, with the appearance of a heat sunk, the radiation parameter improves the decline of the heat transport ratio due to fewer thermal energy being presented in the boundary layer. It is also worth mentioning that when heat is taken from the fluid (heat sinking), the thermal energy component reduces compared to kinetic energy. A more significant Eckert number, paired with heat sinking, can contribute to lower skin friction. This is because the reduced thermal energy component results in less energy available for heat dissipation and frictional losses, resulting in a lower heat transportation ratio. It is eye-catching that the magnetic parameter augmented the skin friction while diminishing the heat transportation ratio. This phenomenon occurs due to the reduction of viscous dissipation, which helps maintain higher kinetic energy in the flow, lowering skin friction and enhancing the heat transportation ratio along the surface.



**Table 6**

Numerical results for skin friction coefficient and Nusselt number for various values of several parameters when  $\alpha = -2.5, S = 2.0, \varphi_1 = 0.01, \varphi_2 = 0.02, \xi = -0.02$ (heat sink) and  $Pr = 6.2$

$M$	$Rd$	$Ec$	$C_f$	$Nu_x$
0.01	0.5	0.1	6.593368584, [0.843041159]	0.716346134, [-5.099046470]
0.03			6.536430282, [0.886452280]	0.742443718, [-4.504436552]
0.04			6.507550743, [0.908656742]	0.755594197, [-4.225334938]
0.03	0.0		6.536430277, [0.886452263]	1.206993868, [-10.181230553]
	0.5		6.536430282, [0.886452280]	0.742443718, [-4.504436552]
	1.0		6.536430278, [0.886452284]	0.534840168, [-2.282368163]
	1.5		6.536430278, [0.886452267]	0.428337686, [-1.282948244]
	1.0	0.1	6.536430278, [0.886452284]	0.534840168, [-2.282368163]
		0.2	6.536430291, [0.886452270]	-4.312986643, [-8.161284740]
		0.3	6.536430294, [0.886452262]	-9.160813453, [-14.040201295]

### 3.2 Velocity and Temperature Profiles

The temperature profile of a fluid system is impacted by several elements, including heat source and heat sink properties as depicted in Figure 2. When the heat source parameter rises, it brings extra thermal energy into the fluid system. The heat source parameter represents a source of heat production inside the fluid. This produced heat adds to raise the temperature of the fluid, especially in the proximity of the heat source. The heat sink parameter, on the other hand, represents a mechanism for heat absorption or dissipation from the fluid system. A decline in the heat sink parameter implies reduce heat absorption or dissipation, allowing extra thermal energy to stay within the fluid. With a decrease heat sink value, there is fewer capacity for the fluid to absorb or disperse heat. This reduces cooling action effects in increased temperatures within the fluid.

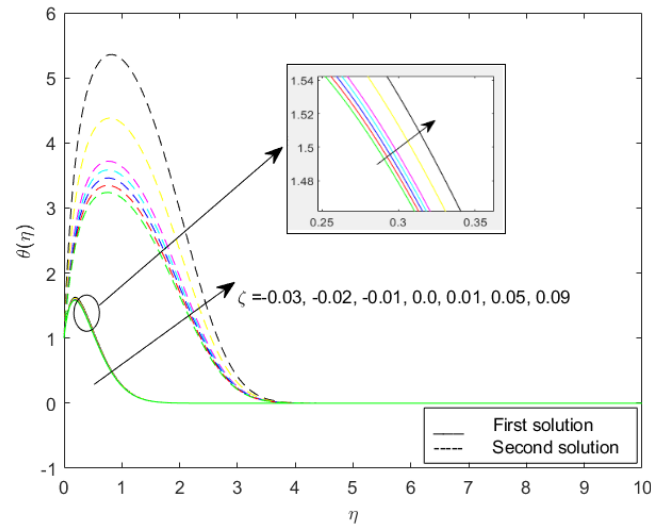


**Fig. 2.** Distribution of temperature profile for several values of heat source and sink when  $M = 0.03$ ,  $Ec = 0.3$ ,  $S = 2.0$ ,  $Pr = 6.2$ ,  $Rd = 1.0$  and ternary hybrid nanofluid parameters  $\phi_1 = 0.01$ ,  $\phi_2 = 0.02$ ,  $\phi_3 = 0.02$

The improve in concentration of GO particles in a fluid flow can modify the fluid's velocity, specifically when forasmuch as the effects of heat source and heat sink influences, as demonstrated in Figure 3. GO particles, specifically at greater amounts, can augment the viscosity of the fluid. This is due to GO particles desire to work together with the fluid molecules, creäte an obstruction to their flow. Additionally, extra substantial concentrations of GO particles can indicate to enhanced thermal conductivity and heat transferal within the fluid in the existence of a heat source. This can affect in restricted temperature adjustments and convective currents, which may alter flow patterns and reduce overall fluid velocity. Contrarywise, a heat sink characteristic illustrates a method for heat dissipation or absorption from the fluid. A decline in the heat sink value implies fewer heat dissipation, indicating to higher temperatures in the fluid. Elevated temperatures could advance thermal expansion of the fluid, which, along with intensified viscosity owing to GO particles, farther reduces fluid flow and velocity.

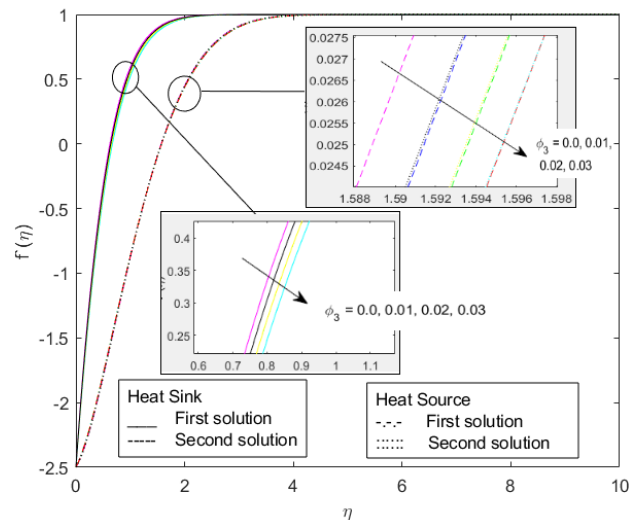


**Fig. 3.** Distribution of velocity profile for several values of GO concentration values when heat source ( $\xi = 0.1$ ), heat sink ( $\xi = -0.03$ ),  $M = 0.03$ ,  $Ec = 0.3$ ,  $S = 2.0$ ,  $Pr = 6.2$ ,  $Rd = 1.0$  and hybrid nanofluid parameters  $\phi_1 = 0.01$ ,  $\phi_2 = 0.02$

The growth in the concentration of GO particles in a fluid flow can initiate the temperature profile of the fluid to expand, as represented in Figure 4. This is specifically valid when taking into account the characteristics of the heat source and heat sink. As the amount of graphene oxide (GO) particles in the fluid grows, the thermal conductivity of the fluid equally improves. Subsequently, the fluid facilitates more efficient heat transfer, causing in raised temperatures in regions involved by the heat source. Intensified concentrations of graphene oxide (GO) particles enhance thermal conduction, allowing the fluid to bring heat away from the heat source zone extra effectively. This can indicate to an extra even dispersion of thermal energy over the fluid, ensuing in a total height of the temperature profile. Contrarywise, an elevated concentration of GO particles can substantially enhance thermal conductivity, making it simpler for heat to move away from locations with minimal temperatures, such as heat sink regions. This can reduce the effectiveness of heat dissipation and provide to raised temperatures in the fluid.

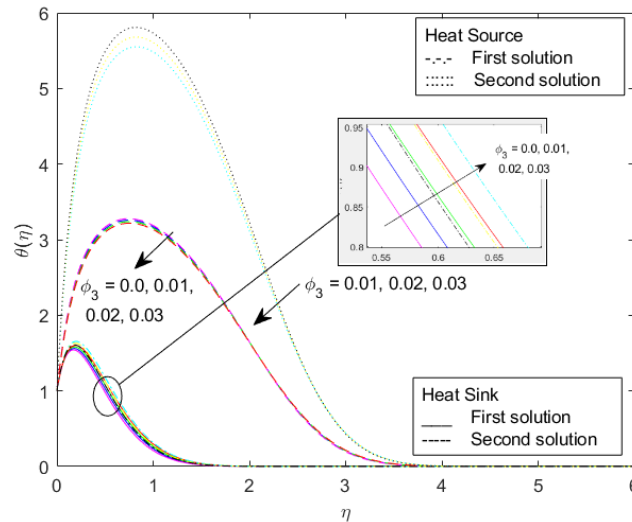


**Fig. 4.** Distribution of temperature profiles for several values of GO concentration when heat source ( $\xi = 0.1$ ), heat sink ( $\xi = -0.03$ ),  $M = 0.03$ ,  $Ec = 0.3$ ,  $S = 2.0$ ,  $Pr = 6.2$ ,  $Rd = 1.0$  and hybrid nanofluid parameters  $\phi_1 = 0.01$ ,  $\phi_2 = 0.02$

#### 4. Conclusions

This research has examined MHD stagnation point flow and heat transfer characteristics of a ternary hybrid nanofluid across a shrinking plate, with a specific emphasis on the influence of radiation and heat generation/absorption. The approach employed in this study entailed the reduction of the governing partial differential equations to ordinary differential equations by the utilisation of similarity transformations. Subsequently, the numerical solution of these ordinary differential equations was obtained utilising the `bvp4c` built-in solver inside the MATLAB program. Hence, the results have yielded significant insights into the impact of several parameters on the features of flow and heat transfer but only restricted to the values tested and with constant radiation effect, as follows:

- i. The net impact is a rise in the temperature profile throughout the fluid system, particularly in locations influenced by the heat source and where heat dissipation is constrained due to lower heat sink capacity.
- ii. The escalation in GO particle concentration in a fluid flow, especially under the impact of heat source and heat sink parameters, leads to increased viscosity, thermal effects and particle interactions, all of which collectively contribute to a reduction in fluid flow velocity.
- iii. The interaction of heat source and heat sink parameters, along with an increased concentration of GO particles, leads to a collective impact on the fluid flow. This results in several combined effects, including improved thermal conductivity, decreased heat dissipation, enhanced convection and frictional heating. As a result, the temperature profile of the fluid experiences an overall increase.

This research can be expanded by considering non-Newtonian ternary hybrid nanofluids, given their extensive applications in various industries. It is advisable to extend the study to optimize the mathematical model and analyse the entropy generation, providing valuable insights into the

utilization and efficiency of the model. Although this study provides a strong foundation for understanding the behaviour of ternary hybrid nanofluids, bridging the gap between theoretical predictions and real-world applications is paramount. Future research should involve comprehensive experimental investigations to validate the numerical results and quantify the performance benefits of ternary hybrid nanofluids under realistic operating conditions. By systematically exploring the effects of key parameters like magnetic field strength, heat source/sink, radiation and suction/injection, researchers can identify optimal configurations for practical applications, such as enhancing heat transfer in heat exchangers and electronic cooling systems. While this study focuses on GO-TiO<sub>2</sub>-Ag/water nanofluid, other combinations, such as those involving Al<sub>2</sub>O<sub>3</sub>, Cu, ZnO or carbon-based nanomaterials, could offer significant advantages. Future research should evaluate these combinations under various conditions to optimize performance and minimize environmental impact, broadening the scope of hybrid nanofluid applications.

### Acknowledgement

The researchers express their gratitude to the Ministry of Higher Education Malaysia, University Putra Malaysia and National Defence University of Malaysia for their valuable supports in facilitating this study. This research was funded by Universiti Putra Malaysia, grant no. GP-IPM 9787700

### References

- [1] Idris, Sakinah, Anuar Jamaludin, Roslinda Nazar and Ioan Pop. "Radiative MHD flow of hybrid nanofluid over permeable moving plate with Joule heating and thermal slip effects." *Alexandria Engineering Journal* 83 (2023): 222-233. <https://doi.org/10.1016/j.aej.2023.09.065>
- [2] Rafique, Khadija, Zafar Mahmood and Umar Khan. "Mathematical analysis of MHD hybrid nanofluid flow with variable viscosity and slip conditions over a stretching surface." *Materials Today Communications* 36 (2023): 106692. <https://doi.org/10.1016/j.mtcomm.2023.106692>
- [3] Mumtaz, Muhammad, Saeed Islam, Hakeem Ullah and Zahir Shah. "Chemically reactive MHD convective flow and heat transfer performance of ternary hybrid nanofluid past a curved stretching sheet." *Journal of Molecular Liquids* 390 (2023): 123179. <https://doi.org/10.1016/j.molliq.2023.123179>
- [4] Mahmood, Zafar, Sayed M. Eldin, Khadija Rafique and Umar Khan. "Numerical analysis of MHD tri-hybrid nanofluid over a nonlinear stretching/shrinking sheet with heat generation/absorption and slip conditions." *Alexandria Engineering Journal* 76 (2023): 799-819. <https://doi.org/10.1016/j.aej.2023.06.081>
- [5] Hussain, Zawar, Fahad Aljuaydi, Muhammad Ayaz and Saeed Islam. "Enhancing thermal efficiency in MHD kerosene oil-based ternary hybrid nanofluid flow over a stretching sheet with convective boundary conditions." *Results in Engineering* 22 (2024): 102151. <https://doi.org/10.1016/j.rineng.2024.102151>
- [6] Jamrus, Farah Nadzirah, Iskandar Waini, Umair Khan and Anuar Ishak. "Effects of magnetohydrodynamics and velocity slip on mixed convective flow of thermally stratified ternary hybrid nanofluid over a stretching/shrinking sheet." *Case Studies in Thermal Engineering* 55 (2024): 104161. <https://doi.org/10.1016/j.csite.2024.104161>
- [7] Ayub, Assad, Muhammad Imran Asjad, Mushrifah AS Al-Malki, Shahzeb Khan, Sayed M. Eldin and Magda Abd El-Rahman. "Scrutiny of nanoscale heat transport with ion-slip and hall current on ternary MHD cross nanofluid over heated rotating geometry." *Case Studies in Thermal Engineering* 53 (2024): 103833. <https://doi.org/10.1016/j.csite.2023.103833>
- [8] Rafique, Khadija, Zafar Mahmood, Umar Khan, Taseer Muhammad, Ahmed Mir, Walid Aich and Lioua Kolsi. "Unsteady MHD flow analysis of hybrid nanofluid over a shrinking surface with porous media and heat generation: Computational study on entropy generation and Bejan number." *International Journal of Heat and Fluid Flow* 107 (2024): 109419. <https://doi.org/10.1016/j.ijheatfluidflow.2024.109419>
- [9] Wahid, Nur Syahirah, Norihan Md Arifin, Rusya Iryanti Yahaya, Najiyah Safwa Khashi'ie and Ioan Pop. "Impact of suction and thermal radiation on unsteady ternary hybrid nanofluid flow over a biaxial shrinking sheet." *Alexandria Engineering Journal* 96 (2024): 132-141. <https://doi.org/10.1016/j.aej.2024.03.079>
- [10] Maranna, T., U. S. Mahabaleswar, L. M. Perez and O. Manca. "Flow of viscoelastic ternary nanofluid over a shrinking porous medium with heat Source/Sink and radiation." *Thermal Science and Engineering Progress* 40 (2023): 101791. <https://doi.org/10.1016/j.tsep.2023.101791>

- [11] Mahabaleshwar, U. S., T. Maranna, L. M. Perez, G. V. Bognar and H. F. Oztop. "An impact of radiation on laminar flow of dusty ternary nanofluid over porous stretching/shrinking sheet with mass transpiration." *Results in Engineering* 18 (2023): 101227. <https://doi.org/10.1016/j.rineng.2023.101227>
- [12] Sharma, Bhupendra K., Parikshit Sharma, Nidhish K. Mishra, Samad Noeiaghdam and Unai Fernandez-Gamiz. "Bayesian regularization networks for micropolar ternary hybrid nanofluid flow of blood with homogeneous and heterogeneous reactions: Entropy generation optimization." *Alexandria Engineering Journal* 77 (2023): 127-148. <https://doi.org/10.1016/j.aej.2023.06.080>
- [13] Aich, Walid, Ghulfam Sarfraz, Nejla Mahjoub Said, Muhammad Bilal, Ahmed Faisal Ahmed Elhag and Ahmed M. Hassan. "Significance of radiated ternary nanofluid for thermal transport in stagnation point flow using thermal slip and dissipation function." *Case Studies in Thermal Engineering* 51 (2023): 103631. <https://doi.org/10.1016/j.csite.2023.103631>
- [14] Ali, Gohar, Poom Kumam, Kanokwan Sitthithakerngkiet and Fahd Jarad. "Heat transfer analysis of unsteady MHD slip flow of ternary hybrid Casson fluid through nonlinear stretching disk embedded in a porous medium." *Ain Shams Engineering Journal* 15, no. 2 (2024): 102419. <https://doi.org/10.1016/j.asej.2023.102419>
- [15] Mahmood, Zafar, Umar Khan, S. Saleem, Khadija Rafique and Sayed M. Eldin. "Numerical analysis of ternary hybrid nanofluid flow over a stagnation region of stretching/shrinking curved surface with suction and Lorentz force." *Journal of Magnetism and Magnetic Materials* 573 (2023): 170654. <https://doi.org/10.1016/j.jmmm.2023.170654>
- [16] Sajid, Tanveer, Wasim Jamshed, Mohamed R. Eid, Salem Algarni, Talal Alqahtani, Rabha W. Ibrahim, Kashif Irshad, Syed M. Hussain and Sayed M. El Din. "Thermal case examination of inconstant heat source (sink) on viscous radiative Sutterby nanofluid flowing via a penetrable rotative cone." *Case Studies in Thermal Engineering* 48 (2023): 103102. <https://doi.org/10.1016/j.csite.2023.103102>
- [17] Sajid, Tanveer, Abdullatif A. Gari, Wasim Jamshed, Mohamed R. Eid, Nazrul Islam, Kashif Irshad, Gilder Cieza Altamirano and Sayed M. El Din. "Case study of autocatalysis reactions on tetra hybrid binary nanofluid flow via Riga wedge: Biofuel thermal application." *Case Studies in Thermal Engineering* 47 (2023): 103058. <https://doi.org/10.1016/j.csite.2023.103058>
- [18] Alqahtani, Aisha M., Muhammad Bilal, Fayza Abdel Aziz Elsebaee, Sayed M. Eldin, Theyab R. Alsenani and Aatif Ali. "Energy transmission through carreau yasuda fluid influenced by ethylene glycol with activation energy and ternary hybrid nanocomposites by using a mathematical model." *Heliyon* 9, no. 4 (2023). <https://doi.org/10.1016/j.heliyon.2023.e14740>
- [19] Alqawasmi, Khaled, Khalid Abdulkhaliq M. Alharbi, Umar Farooq, Sobia Noreen, Muhammad Imran, Ali Akgül, Mohammad Kanan and Jihad Asad. "Numerical approach toward ternary hybrid nanofluid flow with nonlinear heat source-sink and fourier heat flux model passing through a disk." *International Journal of Thermofluids* 18 (2023): 100367. <https://doi.org/10.1016/j.ijft.2023.100367>
- [20] Mishra, Ashish, Sawan Kumar Rawat, Moh Yaseen and Manish Pant. "Development of machine learning algorithm for assessment of heat transfer of ternary hybrid nanofluid flow towards three different geometries: case of artificial neural network." *Heliyon* 9, no. 11 (2023). <https://doi.org/10.1016/j.heliyon.2023.e21453>
- [21] Wahid, Nur Syahirah, Norihan Md Arifin, Ioan Pop, Norfifah Bachok and Mohd Ezad Hafidz Hafidzuddin. "MHD stagnation-point flow of nanofluid due to a shrinking sheet with melting, viscous dissipation and Joule heating effects." *Alexandria Engineering Journal* 61, no. 12 (2022): 12661-12672. <https://doi.org/10.1016/j.aej.2022.06.041>
- [22] Khashi'ie, Najiyah Safwa, Norihan Md Arifin, Roslinda Nazar, Ezad Hafidz Hafidzuddin, Nadiyah Wahi and Ioan Pop. "Mixed convective flow and heat transfer of a dual stratified micropolar fluid induced by a permeable stretching/shrinking sheet." *Entropy* 21, no. 12 (2019): 1162. <https://doi.org/10.3390/e21121162>
- [23] Redouane, Fares, Wasim Jamshed, S. Suriya Uma Devi, M. Prakash, Nor Ain Azeany Mohd Nasir, Zakia Hammouch, Mohamed R. Eid et al., "Heat flow saturate of Ag/MgO-water hybrid nanofluid in heated trigonal enclosure with rotate cylindrical cavity by using Galerkin finite element." *Scientific Reports* 12, no. 1 (2022): 2302. <https://doi.org/10.1038/s41598-022-06134-6>
- [24] Aminuddin, Nur Aisyah, Nor Ain Azeany Mohd Nasir, Wasim Jamshed, Norli Abdullah, Anuar Ishak, Ioan Pop and Mohamed R. Eid. "Velocity and thermal slip impact towards GO-MoS<sub>2</sub>/C<sub>3</sub>H<sub>8</sub>O<sub>3</sub> hybridity nanofluid flowing via a moving Riga plate." *Ain Shams Engineering Journal* 15, no. 4 (2024): 102648. <https://doi.org/10.1016/j.asej.2024.102648>
- [25] Nasir, N. A. A. M., A. Ishak, I. Pop and N. Zainuddin. "MHD stagnation point flow towards a quadratically stretching/shrinking surface." In *Journal of Physics: Conference Series*, vol. 1366, no. 1, p. 012013. IOP Publishing, 2019. <https://doi.org/10.1088/1742-6596/1366/1/012013>

- [26] Akaje, Wasiu and B. I. Olajuwon. "Impacts of Nonlinear thermal radiation on a stagnation point of an aligned MHD Casson nanofluid flow with Thompson and Troian slip boundary condition." *Journal of Advanced Research in Experimental Fluid Mechanics and Heat Transfer* 6, no. 1 (2021): 1-15.
- [27] Kumar, Abhilash Anand, Sreedhar Sobhanapuram and Mangali Veera Krishna. "Nonlinear Mixed Convective Flow of Darcy-Forchheimer Maxwell Tri-Hybrid Nanofluid Past a Riga Plate." *Journal of Advanced Research in Numerical Heat Transfer* 25, no. 1 (2024): 53-72. <https://doi.org/10.37934/arnht.25.1.5372>